Levitated Optomechanics with Meta-Atoms

Sergei Lepeshov,[1] Nadine Meyer,[2,3] Patrick Maurer,[4,5] Oriol Romero-Isart,[4,5,*] and Romain Quidant[2,3,†]
[1]*School of Physics and Engineering, ITMO University, Saint Petersburg, Russia*
[2]*Nanophotonic Systems Laboratory, Department of Mechanical and Process Engineering, ETH Zurich, 8092 Zurich, Switzerland*
[3]*Quantum Center, ETH Zurich, 8083 Zurich, Switzerland*
[4]*Institute for Quantum Optics and Quantum Information of the Austrian Academy of Sciences, A-6020 Innsbruck, Austria*
[5]*Institute for Theoretical Physics, University of Innsbruck, A-6020 Innsbruck, Austria*

(Received 30 November 2022; accepted 10 May 2023; published 8 June 2023)

We propose to introduce additional control in levitated optomechanics by trapping a meta-atom, i.e., a subwavelength and high-permittivity dielectric particle supporting Mie resonances. In particular, we theoretically demonstrate that optical levitation and center-of-mass ground-state cooling of silicon nanoparticles in vacuum is not only experimentally feasible but it offers enhanced performance over widely used silica particles in terms of trap frequency, trap depth, and optomechanical coupling rates. Moreover, we show that, by adjusting the detuning of the trapping laser with respect to the particle's resonance, the sign of the polarizability becomes negative, enabling levitation in the minimum of laser intensity, e.g., at the nodes of a standing wave. The latter opens the door to trapping nanoparticles in the optical near-field combining red and blue-detuned frequencies, in analogy to two-level atoms, which is of interest for generating strong coupling to photonic nanostructures and short-distance force sensing.

DOI: 10.1103/PhysRevLett.130.233601

Optical trapping and motional control of polarizable submicron objects in vacuum has become a very active research field [1,2]. Recently, the motion of an optically levitated silica nanoparticle has been cooled to the quantum ground state, either using passive feedback cooling via coherent scattering into a cavity [3–5], or via active feedback cooling [6–8] with shot-noise limited optical detection. In addition, the optical dipole-dipole interaction between two silica nanoparticles trapped in vacuum in two separate optical tweezers has been measured [9], which opens the door to study many-particle physics in vacuum [2,10–16]. Optical trapping and control in vacuum of more complex particles supporting internal resonances has thus far been considered unattainable due to laser absorption, and has been solely studied by using low frequency electric [17–20] or magnetic fields [20–28]. In contrast to optical manipulation, magnetic and electric platforms are less advanced and face additional challenges in terms of motional control in the quantum regime [2].

In this Letter, we analyze the use of Mie resonances supported by silicon nanoparticles [29] for optical levitation in vacuum [30]. We demonstrate that the resonances enable larger trap frequencies and trap depths compared to silica nanoparticles. Remarkably, we also evidence that silicon nanoparticles of few hundred nanometers behave, from the optomechanical standpoint, as a meta-atom whose polarizability changes sign across the resonance. In analogy with two-level atoms, this enables trapping the particle in regions of minimum laser intensity [31–34]. The frequency-dependent sign of the polarizability is foreseen to enable trapping of silicon particles near a surface by using two-color near-field traps [35,36]. The latter is of interest to couple particle's motion to optical microcavities [37] or other integrated photonic systems [38–40]. In the context of optical interaction of many particles, optical resonances pave the way to engineer stronger and more complex types of interactions beyond dipole-dipole interaction. Last but not least, in the context of levitated optomechanics, we theoretically show how to achieve motional ground-state cooling of optically resonant nanoparticles and discuss its distinctive features, including larger cooling rates and even the possibility of entering the strong optomechanical coupling regime in free space [3,41,42].

Let us consider a spherical silicon (Si) particle of radius R, mass m, and homogeneous refractive index $n = n_r + in_i$, interacting with laser light in ultrahigh vacuum. We consider a standing wave pattern along the z axis that is formed by two x-polarized and counter-propagating focused laser beams of equal wavelength λ, and with a relative phase $\Delta\phi$ [43–46] (Fig. 1). The case $\Delta\phi = 0$ and $\Delta\phi = \pi$ corresponds to the optical configuration with constructive interference and destructive interference at the focal point, respectively. Because of the symmetry of the illumination, the scattering forces experienced by the particle cancel out such that trapping conditions are fully determined by both field intensity gradients and particle polarizability. Unlike subwavelength silica (SiO_2) nanoparticles that behave as nonresonant dipole scatterers, a subwavelength Si nanoparticle supports

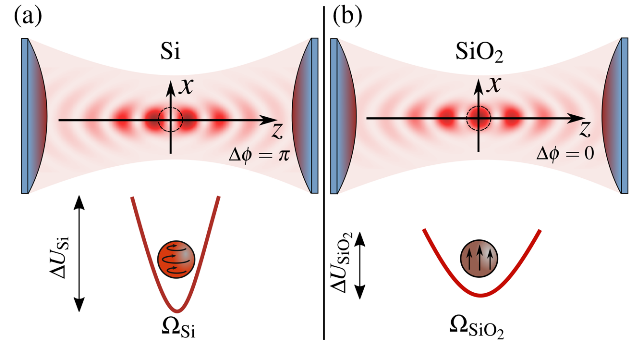

FIG. 1. Illustration of the optical configuration and the corresponding optical potential with trap depth ΔU and trap frequency Ω. In both panels the optical configuration consists of two x-polarized focused laser beams of equal wavelength, counter-propagating along the z axis. The relative phase $\Delta\phi$ specifies the intensity of the standing wave at the focal point. (a) Silicon nanosphere trapped at the intensity minimum ($\Delta\phi = \pi$) (b) Silica nanosphere trapped at the intensity maximum ($\Delta\phi = 0$).

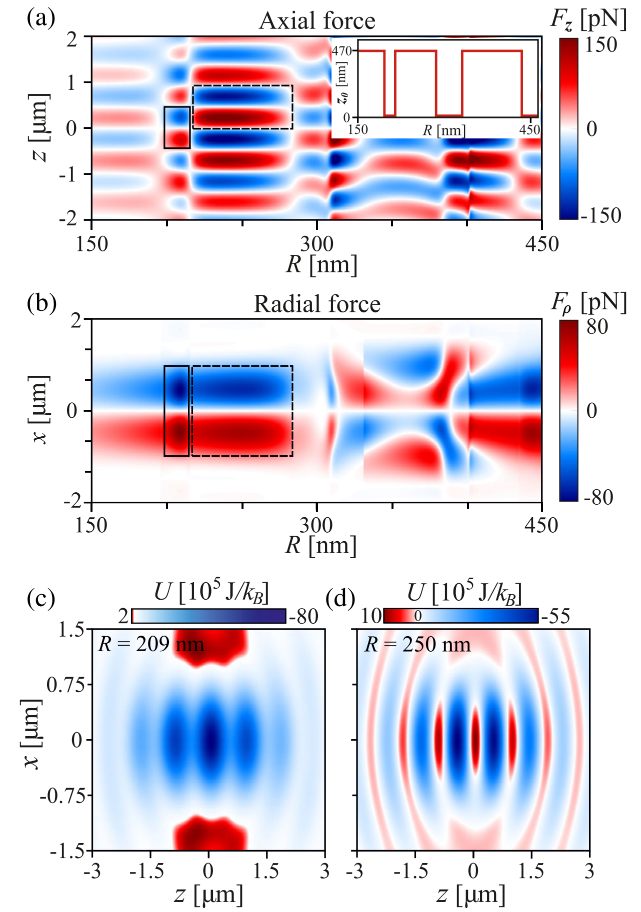

FIG. 2. (a) Axial force $F_z(0, 0, z)$ as a function of axial distance z and radius R for $\Delta\phi = \pi$ (dark focal spot). Inset shows the axial trapping position z_0 as a function of radius R. The corresponding ranges $R[\mathrm{nm}] \approx (196, 215)$ and $R[\mathrm{nm}] \approx (216, 284)$ are highlighted by solid and dashed black boxes in (a) and (b). (b) Radial force $F_\rho(x, 0, z_0)$ as a function of the radial distance x, radius R, and z_0 as specified in the inset of (a). (c) Optical potential U for Si nanoparticles with $R = 209$ nm trapped at the dark focal point $z_0 = 0$. (d) Optical potential for Si nanoparticles with $R = 250$ nm trapped at the bright spot $z_0 \neq 0$.

multipolar Mie resonances [29] whose spectral features depend on the real part of the dielectric constant $\epsilon = n^2$ and the ratio R/λ. The enhanced nanoparticle polarizability at a given Mie resonance is expected to substantially increase the total force experienced by the particle, and thereby to increase trap depth and trap frequencies compared to a SiO_2 nanoparticle (Fig. 1). Furthermore, as discussed later, Mie resonances offer an opportunity to control the sign of the force by an appropriate detuning between the Mie resonance and the frequency of the trapping laser, thereby enabling the trapping of particles at a dark spot [Fig. 1(a)].

To test these hypotheses, we use the optical tweezers computational toolbox [47] to calculate the total optical force on a Si nanoparticle with center-of-mass position $\mathbf{r}$ in the standing-wave configuration described above. We set the focal point of the standing wave at $z = 0$ (Fig. 1). Hereafter, we make use of the paraxial approximation such that the optical force acting on a particle placed near the focus has cylindrical symmetry [48]. Hence, the total force is characterized by a force term along the standing-wave axis, denoted by $F_z(\mathbf{r})$, and a force term perpendicular to the optical axis, denoted by $F_\rho(\mathbf{r})$. In Fig. 2(a) we plot $F_z(0, 0, z)$ as a function of radius R and axial distance z for $\Delta\phi = \pi$ (dark focal spot) and using the experimental parameters given in Table I. Note that, $F_z(0, 0, z)$ changes its sign multiple times both as a function of z due to the standing-wave profile and, remarkably, as a function of radius R as the trapping wavelength swipes across the different Mie resonances. Similar sign flips are observed for the radial force F_ρ as a function of radius R and radial distance x; see Fig. 2(b). For $\Delta\phi = 0$ (bright focal spot) the axial force $F_z(0, 0, z)$ displays opposite attractive and repulsive regions while the radial force remains unchanged; see Ref. [49]. Overall three-dimensional trapping can be achieved in the dark, where, in absence of the particle, light destructively interferes. As seen from the map of the optical potential $U(\mathbf{r})$ displayed in Figs. 2(c) and 2(d), the axial trapping position z_0 occurs either at the focal dark point $z_0 = 0$ for radii in the range $R[\mathrm{nm}] \approx (196, 215)$ and in a neighboring bright spot for radii in the range $R[\mathrm{nm}] \approx (216, 284)$ [these radii ranges are highlighted by the black boxes in Figs. 2(a) and 2(b)]. Hereafter, we will exclusively consider optical trapping at the focal point $z_0 = 0$, which requires using either $\Delta\phi = \pi$ (dark trapping) or $\Delta\phi = 0$ (bright trapping) configuration depending on the particle size.

In particle trapping, both the trap depth ΔU and the trap frequencies Ω_z and Ω_ρ are key parameters to quantify the quality of the trap. The trap depth ΔU is defined as the kinetic motional energy required for the particle to escape. The trap frequencies Ω_z and Ω_ρ are defined when the

TABLE I. Table of proposed experimental parameters.

Parameters	Description
$\lambda = 1550$ nm	Laser wavelength
P = 50 mW	Laser power per beam
NA = 0.8	Numerical aperture
$n_{\mathrm{Si}}(\lambda) = 3.48 + \mathrm{i}\,5.3038 \times 10^{-11}$	Refractive index of Si [55]
$n_{\mathrm{SiO_2}}(\lambda) = 1.46 + \mathrm{i}\,5 \times 10^{-9}$	Refractive index of SiO_2 [56]
$\rho_{\mathrm{Si}} = 2330\ \mathrm{kg\,m^{-3}}$	Mass density of Si
$\rho_{\mathrm{SiO_2}} = 2200\ \mathrm{kg\,m^{-3}}$	Mass density of SiO_2

optical potential is expanded around its minimum (in our case, near the focus), namely $U(\mathbf{r}) \approx m\Omega_z^2 z^2/2 + m\Omega_\rho^2 \rho^2/2$. In levitated optomechanics, the mechanical trap frequency along a given axis sets an important timescale for the dynamics. In the quantum regime, the trap frequency is required to be larger than the decoherence rate caused by any noise source other than laser recoil heating. Maximizing trap frequencies is thus desirable for bringing the motion of a particle into the quantum regime. In Fig. 3(a) we plot ΔU and in Fig. 3(b) Ω_z and Ω_ρ as a function of radius R for a particle trapped at $z_0 = 0$ (the upper horizontal axis shows whether the dark $\Delta\phi = \pi$ or bright $\Delta\phi = 0$ configuration is required). For comparison, we also display with the dashed line the case of a SiO_2 nanoparticle for the bright configuration $\Delta\phi = 0$, which is the only possibility to trap a nonresonant dielectric particle. In contrast to what is observed for SiO_2, ΔU and $\Omega_{z,\rho}$ display for Si complex R dependence with regions of both enhancement and diminution. The maximum trap depth is achieved for $R = 209$ nm in the dark trapping and for $R = 250$ nm in the bright trapping (black dotted lines), with trap depths approximately 25 times greater than for SiO_2. Both axial Ω_z and radial Ω_ρ mechanical frequencies also display enhanced values, which can be more than 5 times larger than those of a SiO_2 nanoparticle. Let us remark that the complex features of Figs. 3(a) and 3(b) correlate to the different electric and magnetic modes supported by the particle [57], as we show in [49].

While so far we have focused on conservative dynamics, namely on the optical potential, the interaction of a dielectric particle with laser light also induces dissipative motional dynamics, i.e., laser light recoil heating [58–60]. Recoil heating induces a linear in time increase of center-of-mass energy due to the backaction caused by the scattered light that carries information about the center-of-mass position. The recoil heating rate Γ_μ along the μ axis ($\mu = x,\ y,\ z$) is defined as $\partial_t E_\mu(t) = \Gamma_\mu \hbar \Omega_\mu$, where $E_\mu(t) = \langle p_\mu^2/(2m) + m\Omega_\mu^2 r_\mu^2/2 \rangle$. The expected value represents an ensemble average over trajectories. In the context of quantum ground-state cooling of the center-of-mass motion of a dielectric particle via optical detection, recoil heating is of paramount importance. Figure 3 shows $\Gamma_{x,z}$ for Si (solid) and SiO_2 (dashed) particles as a function of radius R calculated using recent theoretical methods [60]. We observe a complex behavior for Si particles, while SiO_2 shows smooth trends expected for particles in the Rayleigh

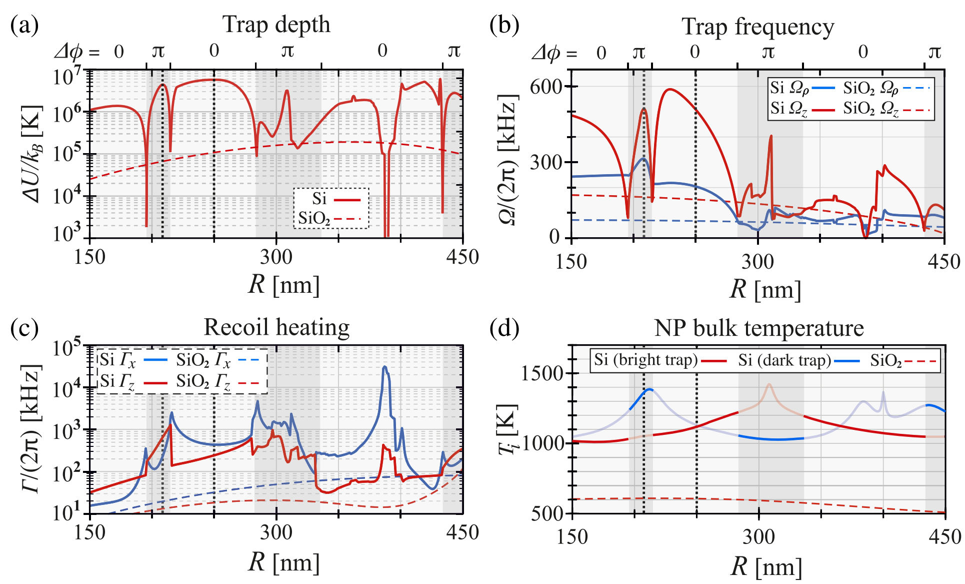

FIG. 3. (a) Trap depth ΔU for $z_0 = 0$ as a function of the radius R for Si (solid) and SiO_2 (dashed). The upper abscissa specifies which relative phase $\Delta\phi$ is used to achieve $z_0 = 0$ for Si. The black dotted lines represent the maximal trap depth at $R \approx 209$ nm (dark), and $R \approx 250$ nm (bright), respectively. (b) Radial trap frequency Ω_ρ (blue) and axial trap frequency Ω_z (red) as a function of the radius R for Si (solid) and SiO_2 (dashed). (c) Recoil heating rate Γ_x along x (blue) and recoil heating rate Γ_z along z (red) as a function of radius R for Si (solid) and SiO_2 (dashed). (d) Internal temperature T_i as a function of radius R for Si in the bright trap (solid red), Si in the dark trap (solid blue), and SiO_2 in the bright trap (red dashed).

regime. In general, $\Gamma_{x,z}$ for Si exceeds SiO_2 for nearly all radii by up to 3 orders of magnitude. This increase is more pronounced for the axial direction. On one hand, higher $\Gamma_{x,z}$ leads to increased decoherence rates at equal power levels. On the other hand, this enhancement implies that more scattered photons carrying information about the particle position are collected, which is advantageous for active feedback cooling, as discussed below. Last but not least, we observe configurations in which $\Gamma_{x,z}$ is comparable or even larger than the trap frequencies, which is a signal of the strong optomechanical coupling regime. The possibility of entering and exploiting the strong optomechanical regime in free space (i.e., without cavities) will be further investigated elsewhere.

Another critical parameter that determines the experimental feasibility of trapping in vacuum is the internal heating of the particle by laser absorption. Thus, it is important to estimate the particle's internal temperature T_i in the different optical trapping configurations under consideration. T_i in high vacuum is estimated by balancing the absorbed laser power and the power emitted by the nanoparticle, which can be calculated using Mie solutions [61–63]; see Ref. [49] for more details. In Fig. 3(d), we show T_i for a Si nanoparticle (solid) in the bright trapping (red) and dark trapping (blue) configuration as a function of radius R for the experimental numbers given in Table I. We observe three local maxima in T_i of the Si nanoparticle that align with excited Mie resonances of a different order; see Ref. [49]. We notice that maximal values of $\Gamma_{x,z}$ coincide with increased T_i. While Si nanoparticles heat up more (around a factor of 2) than SiO_2 nanoparticles (dashed line), the internal temperature is lower than the melting point of bulk Si (≈1700 K).

Let us now show that motional ground state cooling of a Si nanoparticle is experimentally feasible, especially in the dark trapping configuration. Assuming that laser recoil is the dominant source of motional heating, phonon occupation along a given axis, say the optical axis, n_z, is only governed by the detection efficiency η, with $n_z = (\sqrt{1/\eta} - 1)/2 < 1$ [6,7,64]. η is the ratio of detected photons that are scattered from the particle by either increasing or decreasing the center-of-mass kinetic energy along the z axis. Hence, it is key to know the angular dependence of such scattered photons to evaluate the portion of them that can be detected and processed by the experimental configuration. This information is given by the so-called radiation patterns [64], calculated using recent theoretical methods [60]. Figure 4 displays the radiation pattern associated with the motion along the z axis in the $x-z$ plane for a Si nanoparticle in a dark (blue solid) and a SiO_2 nanoparticle in a bright trap (red dashed), and equal radii $R = 209$ nm. It illustrates that, under our conditions, scattered photons feature a very similar angular pattern. The gray shaded area illustrates the collected light fraction governed by the NA. For NA > 0.75, the reached detection efficiencies are equal

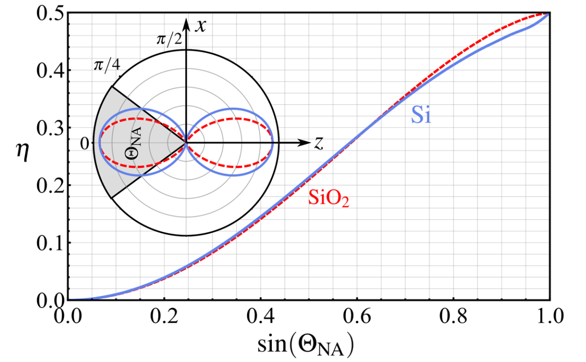

FIG. 4. Detection efficiency η along z as a function of the numerical aperture $\mathrm{NA} = \sin\Theta_{\mathrm{NA}}$ for Si (solid blue) and SiO_2 (dashed red) at $R = 209$ nm. Inset shows the (normalized) information radiation pattern along z in the x-z plane for both Si (solid blue) and SiO_2 (dashed red).

for both scenarios, and for NA = 0.8 the detection efficiency yields $\eta = 0.41$ for Si and $\eta = 0.42$ for SiO_2. Hence, ground state cooling with $n = 0.28$ is in reach, as already demonstrated for bright traps in [6,7]. Let us emphasize that recoil heating for Si nanoparticles is up to 3 orders of magnitude larger than for SiO_2 implying that ground-state cooling can be achieved either with 3 orders of magnitude faster timescale or with up to 3 orders of magnitude less laser power. In the regimes where the recoil heating rates are comparable or larger than the trapping frequencies, other cooling methods based on the use of light pulses could be employed [65].

In summary, we have shown how Mie resonances in silicon nanoparticles introduce an additional degree of control over the dynamics of levitated mechanical oscillators. First, the higher mechanical frequencies, trap depths, and recoil heating rates, as compared to standard silica particles, contribute to increased motional quantum control of nanoparticles. Second, the sign change of the particle's polarizability with the laser frequency enables trapping and center-of-mass ground-state cooling at a laser intensity minimum. We foresee that these unique properties of levitated meta-atoms will open new opportunities in levitodynamics [2], inspired by atom optics. In particular, multiwavelength trapping should enable the accurate control of the distance to an interface [35], critical to the study of surface forces [66], and coupling to photonic structures [67]. Furthermore, parallel trapping of silicon meta-atoms would allow the exploration of interactions beyond the dipole-dipole regime through higher order multipoles, such as electric or magnetic quadrupoles.

We acknowledge valuable discussions with Yuri Kivshar, Ivan Toftul and Massimiliano Rossi. S. L. acknowledges support of Priority 2030 Federal Academic Leadership Program. This research was supported by the European Research Council (ERC) under the grant Agreement No. [951234] (Q-Xtreme ERC-2020-SyG).

*Corresponding author.
Oriol.Romero-Isart@uibk.ac.at
†Corresponding author.
rquidant@ethz.ch

[1] J. Millen, T. S. Monteiro, R. Pettit, and A. N. Vamivakas, Optomechanics with levitated particles, Rep. Prog. Phys. **83**, 026401 (2020).
[2] C. Gonzalez-Ballestero, M. Aspelmeyer, L. Novotny, R. Quidant, and O. Romero-Isart, Levitodynamics: Levitation and control of microscopic objects in vacuum, Science **374** (2021).
[3] U. Delić, M. Reisenbauer, K. Dare, D. Grass, V. Vuletić, N. Kiesel, and M. Aspelmeyer, Cooling of a levitated nanoparticle to the motional quantum ground state, Science **367**, 892 (2020).
[4] A. Ranfagni, K. Børkje, F. Marino, and F. Marin, Two-dimensional quantum motion of a levitated nanosphere, Phys. Rev. Res. **4**, 033051 (2022).
[5] J. Piotrowski, D. Windey, J. Vijayan, C. Gonzalez-Ballestero, A. de los Ríos Sommer, N. Meyer, R. Quidant, O. Romero-Isart, R. Reimann, and L. Novotny, Simultaneous ground-state cooling of two mechanical modes of a levitated nanoparticle, Nat. Phys. (2023), 10.1038/s41567-023-01956-1.
[6] F. Tebbenjohanns, M. L. Mattana, M. Rossi, M. Frimmer, and L. Novotny, Quantum control of a nanoparticle optically levitated in cryogenic free space, Nature (London) **595**, 378 (2021).
[7] L. Magrini, P. Rosenzweig, C. Bach, A. Deutschmann-Olek, S. G. Hofer, S. Hong, N. Kiesel, A. Kugi, and M. Aspelmeyer, Real-time optimal quantum control of mechanical motion at room temperature, Nature (London) **595**, 373 (2021).
[8] M. Kamba, R. Shimizu, and K. Aikawa, Optical cold damping of neutral nanoparticles near the ground state in an optical lattice, Opt. Express **30**, 26716 (2022).
[9] J. Rieser, M. A. Ciampini, H. Rudolph, N. Kiesel, K. Hornberger, B. A. Stickler, M. Aspelmeyer, and U. Delić, Tunable light-induced dipole-dipole interaction between optically levitated nanoparticles, Science **377**, 987 (2022).
[10] D. R. Burnham and D. McGloin, Holographic optical trapping of aerosol droplets, Opt. Express **14**, 4175 (2006).
[11] K. Dholakia and P. Zemánek, Colloquium: Gripped by light: Optical binding, Rev. Mod. Phys. **82**, 1767 (2010).
[12] W. Lechner, S. J. M. Habraken, N. Kiesel, M. Aspelmeyer, and P. Zoller, Cavity Optomechanics of Levitated Nanodumbbells: Nonequilibrium Phases and Self-Assembly, Phys. Rev. Lett. **110**, 143604 (2013).
[13] S. Liu, Z.-q. Yin, and T. Li, Prethermalization and nonreciprocal phonon transport in a levitated optomechanical array, Adv. Quantum Technol. **3**, 1900099 (2020).
[14] J. Yan, X. Yu, Z. V. Han, T. Li, and J. Zhang, On-demand assembly of optically-levitated nanoparticle arrays in vacuum, arXiv:2207.03641.
[15] P. Verkerk, B. Lounis, C. Salomon, C. Cohen-Tannoudji, J.-Y. Courtois, and G. Grynberg, Dynamics and Spatial Order of Cold Cesium Atoms in a Periodic Optical Potential, Phys. Rev. Lett. **68**, 3861 (1992).
[16] P. S. Jessen, C. Gerz, P. D. Lett, W. D. Phillips, S. L. Rolston, R. J. C. Spreeuw, and C. I. Westbrook, Observation of Quantized Motion of Rb Atoms in an Optical Field, Phys. Rev. Lett. **69**, 49 (1992).
[17] P. Z. G. Fonseca, E. B. Aranas, J. Millen, T. S. Monteiro, and P. F. Barker, Nonlinear Dynamics and Strong Cavity Cooling of Levitated Nanoparticles, Phys. Rev. Lett. **117**, 173602 (2016).
[18] G. P. Conangla, A. W. Schell, R. A. Rica, and R. Quidant, Motion control and optical interrogation of a levitating single nitrogen vacancy in vacuum, Nano Lett. **18**, 3956 (2018).
[19] G. P. Conangla, R. A. Rica, and R. Quidant, Extending vacuum trapping to absorbing objects with hybrid paul-optical traps, Nano Lett. **20**, 6018 (2020).
[20] T. Delord, P. Huillery, L. Nicolas, and G. Hétet, Spin-cooling of the motion of a trapped diamond, Nature (London) **580**, 56 (2020).
[21] T. Wang, S. Lourette, S. R. O'Kelley, M. Kayci, Y. B. Band, D. F. J. Kimball, A. O. Sushkov, and D. Budker, Dynamics of a Ferromagnetic Particle Levitated over a Superconductor, Phys. Rev. Appl. **11**, 044041 (2019).
[22] C. Timberlake, G. Gasbarri, A. Vinante, A. Setter, and H. Ulbricht, Acceleration sensing with magnetically levitated oscillators above a superconductor, Appl. Phys. Lett. **115**, 224101 (2019).
[23] A. Vinante, P. Falferi, G. Gasbarri, A. Setter, C. Timberlake, and H. Ulbricht, Ultralow Mechanical Damping with Meissner-Levitated Ferromagnetic Microparticles, Phys. Rev. Appl. **13**, 064027 (2020).
[24] J. Gieseler, A. Kabcenell, E. Rosenfeld, J. D. Schaefer, A. Safira, M. J. A. Schuetz, C. Gonzalez-Ballestero, C. C. Rusconi, O. Romero-Isart, and M. D. Lukin, Single-Spin Magnetomechanics with Levitated Micromagnets, Phys. Rev. Lett. **124**, 163604 (2020).
[25] C. W. Lewandowski, T. D. Knowles, Z. B. Etienne, and B. D'Urso, High-Sensitivity Accelerometry with a Feedback-Cooled Magnetically Levitated Microsphere, Phys. Rev. Appl. **15**, 014050 (2021).
[26] M. G. Latorre, A. Paradkar, D. Hambraeus, G. Higgins, and W. Wieczorek, A chip-based superconducting magnetic trap for levitating superconducting microparticles, IEEE Trans. Appl. Supercond. **32**, 1 (2022).
[27] M. G. Latorre, G. Higgins, A. Paradkar, T. Bauch, and W. Wieczorek, Superconducting microsphere magnetically levitated in an anharmonic potential, arXiv:2210.13451.
[28] O. Romero-Isart, L. Clemente, C. Navau, A. Sanchez, and J. I. Cirac, Quantum Magnetomechanics with Levitating Superconducting Microspheres, Phys. Rev. Lett. **109**, 147205 (2012).
[29] C. Zhang, Y. Xu, J. Liu, J. Li, J. Xiang, H. Li, J. Li, Q. Dai, S. Lan, and A. E. Miroshnichenko, Lighting up silicon nanoparticles with mie resonances, Nat. Commun. **9**, 2964 (2018).
[30] A. Ashkin and J. M. Dziedzic, Observation of Resonances in the Radiation Pressure on Dielectric Spheres, Phys. Rev. Lett. **38**, 1351 (1977).
[31] R. Grimm, M. Weidemüller, and Y. B. Ovchinnikov, *Optical Dipole Traps for Neutral Atoms*, Advances In Atomic, Molecular, and Optical Physics Vol. 42 (Academic Press, New York, 2000), pp. 95–170, 10.1016/S1049-250X(08)60186-X.
[32] A. Kaplan, N. Friedman, and N. Davidson, Optimized single-beam dark optical trap, J. Opt. Soc. Am. B **19**, 1233 (2002).

[33] A. Jaouadi, N. Gaaloul, B. Viaris de Lesegno, M. Telmini, L. Pruvost, and E. Charron, Bose-Einstein condensation in dark power-law laser traps, Phys. Rev. A **82**, 023613 (2010).

[34] M. L. Juan, G. Molina-Terriza, T. Volz, and O. Romero-Isart, Near-field levitated quantum optomechanics with nanodiamonds, Phys. Rev. A **94**, 023841 (2016).

[35] F. Le Kien, V. I. Balykin, and K. Hakuta, Atom trap and waveguide using a two-color evanescent light field around a subwavelength-diameter optical fiber, Phys. Rev. A **70**, 063403 (2004).

[36] E. Vetsch, D. Reitz, G. Sagué, R. Schmidt, S. T. Dawkins, and A. Rauschenbeutel, Optical Interface Created by Laser-Cooled Atoms Trapped in the Evanescent Field Surrounding an Optical Nanofiber, Phys. Rev. Lett. **104**, 203603 (2010).

[37] K. J. Vahala, Optical microcavities, Nature (London) **424**, 839 (2003).

[38] Y. Akahane, T. Asano, B.-S. Song, and S. Noda, High-q photonic nanocavity in a two-dimensional photonic crystal, Nature (London) **425**, 944 (2003).

[39] P. B. Deotare, M. W. McCutcheon, I. W. Frank, M. Khan, and M. Lončar, High quality factor photonic crystal nanobeam cavities, Appl. Phys. Lett. **94**, 121106 (2009).

[40] L. Magrini, R. A. Norte, R. Riedinger, I. Marinković, D. Grass, U. Delić, S. Gröblacher, S. Hong, and M. Aspelmeyer, Near-field coupling of a levitated nanoparticle to a photonic crystal cavity, Optica **5**, 1597 (2018).

[41] A. Ranfagni, P. Vezio, M. Calamai, A. Chowdhury, F. Marino, and F. Marin, Vectorial polaritons in the quantum motion of a levitated nanosphere, Nat. Phys. **17**, 1120 (2021).

[42] A. de los Ríos Sommer, N. Meyer, and R. Quidant, Strong optomechanical coupling at room temperature by coherent scattering, Nat. Commun. **12**, 276 (2021).

[43] T. Čižmár, V. Garcés-Chávez, K. Dholakia, and P. Zemánek, Optical conveyor belt for delivery of submicron objects, Appl. Phys. Lett. **86**, 174101 (2005).

[44] O. Brzobohatý, V. Karásek, M. Šiler, L. Chvátal, T. Čižmár, and P. Zemánek, Experimental demonstration of optical transport, sorting and self-arrangement using a 'tractor beam', Nat. Photonics **7**, 123 (2013).

[45] D. Grass, J. Fesel, S. G. Hofer, N. Kiesel, and M. Aspelmeyer, Optical trapping and control of nanoparticles inside evacuated hollow core photonic crystal fibers, Appl. Phys. Lett. **108**, 221103 (2016).

[46] M. Nikkhou, Y. Hu, J. A. Sabin, and J. Millen, Direct and clean loading of nanoparticles into optical traps at millibar pressures, Photonics **8**, 458 (2021).

[47] T. A. Nieminen, V. L. Loke, A. B. Stilgoe, G. Knöner, A. M. Brańczyk, N. R. Heckenberg, and H. Rubinsztein-Dunlop, Optical tweezers computational toolbox, J. Opt. A **9**, S196 (2007).

[48] L. Novotny and B. Hecht, *Principles of Nano-Optics* (Cambridge University Press, Cambridge, England, 2012).

[49] See Supplemental Material at http://link.aps.org/supplemental/10.1103/PhysRevLett.130.233601, which includes the Refs. [50–54], for more details on the trap characterization, the effective particle polarizability, Mie scattering and absorption cross section and the derivation of the internal temperature of the particle.

[50] J. Chen, J. Ng, Z. Lin, and C. T. Chan, Optical pulling force, Nat. Photonics **5**, 531 (2011).

[51] A. B. Evlyukhin, T. Fischer, C. Reinhardt, and B. N. Chichkov, Optical theorem and multipole scattering of light by arbitrarily shaped nanoparticles, Phys. Rev. B **94**, 205434 (2016).

[52] Ø. Farsund and B. Felderhof, Force, torque, and absorbed energy for a body of arbitrary shape and constitution in an electromagnetic radiation field, Physica A (Amsterdam) **227**, 108 (1996).

[53] C. Schinke, P. Christian Peest, J. Schmidt, R. Brendel, K. Bothe, M. R. Vogt, I. Kröger, S. Winter, A. Schirmacher, S. Lim *et al.*, Uncertainty analysis for the coefficient of band-to-band absorption of crystalline silicon, AIP Adv. **5**, 067168 (2015).

[54] D. Chandler-Horowitz and P. M. Amirtharaj, High-accuracy, midinfrared ($450\ \mathrm{cm}^{-1} \leq \omega \leq 4000\ \mathrm{cm}^{-1}$) refractive index values of silicon, J. Appl. Phys. **97**, 123526 (2005).

[55] J. Degallaix, R. Flaminio, D. Forest, M. Granata, C. Michel, L. Pinard, T. Bertrand, and G. Cagnoli, Bulk optical absorption of high resistivity silicon at 1550 nm, Opt. Lett. **38**, 2047 (2013).

[56] E. D. Palik, *Handbook of Optical Constants of Solids* (Academic Press, New York, 1998), Vol. 3.

[57] Y. Kivshar and A. Miroshnichenko, Meta-optics with mie resonances, Opt. Photonics News **28**, 24 (2017).

[58] V. Jain, J. Gieseler, C. Moritz, C. Dellago, R. Quidant, and L. Novotny, Direct Measurement of Photon Recoil from a Levitated Nanoparticle, Phys. Rev. Lett. **116**, 243601 (2016).

[59] C. Gonzalez-Ballestero, P. Maurer, D. Windey, L. Novotny, R. Reimann, and O. Romero-Isart, Theory for cavity cooling of levitated nanoparticles via coherent scattering: Master equation approach, Phys. Rev. A **100**, 013805 (2019).

[60] P. Maurer, C. Gonzalez-Ballestero, and O. Romero-Isart, Quantum theory of light interaction with a dielectric sphere: Towards 3D ground-state cooling, arXiv:2212.04838.

[61] C. F. Bohren and D. R. Huffman, *Absorption and Scattering of Light by Small Particles* (John Wiley & Sons, New York, 2008).

[62] L. Landström and P. Heszler, Analysis of blackbody-like radiation from laser-heated gas-phase tungsten nanoparticles, J. Phys. Chem. B **108**, 6216 (2004).

[63] J. Bateman, S. Nimmrichter, K. Hornberger, and H. Ulbricht, Near-field interferometry of a free-falling nanoparticle from a point-like source, Nat. Commun. **5**, 1 (2014).

[64] F. Tebbenjohanns, M. Frimmer, and L. Novotny, Optimal position detection of a dipolar scatterer in a focused field, Phys. Rev. A **100**, 043821 (2019).

[65] J. S. Bennett, K. Khosla, L. S. Madsen, M. R. Vanner, H. Rubinsztein-Dunlop, and W. P. Bowen, A quantum optomechanical interface beyond the resolved sideband limit, New J. Phys. **18**, 053030 (2016).

[66] A. A. Geraci, S. B. Papp, and J. Kitching, Short-Range Force Detection Using Optically Cooled Levitated Microspheres, Phys. Rev. Lett. **105**, 101101 (2010).

[67] P. Forn-Díaz, L. Lamata, E. Rico, J. Kono, and E. Solano, Ultrastrong coupling regimes of light-matter interaction, Rev. Mod. Phys. **91**, 025005 (2019).